Supporting Information for

Local Structures and Catalytic Ammonia Combustion Properties of Copper Oxides and Silver Supported on Aluminum Oxides

Satoshi Hinokuma*[†‡], Yusuke Kawabata[†], Shun Matsuki[†], Hiroki Shimanoe[†], Saaya Kiritoshi[†], and Masato Machida[†]

[†] *Department of Applied Chemistry and Biochemistry, Graduate School of Science and Technology, Kumamoto University, 2-39-1 Kurokami, Chuo-ku, Kumamoto 860-8555, Japan*

[‡] *Japan Science and Technology Agency, Precursory Research for Embryonic Science and Technology, 4-1-8 Honcho, Kawaguchi, Saitama, 332-0012, Japan*

E-mail: hinokuma@kumamoto-u.ac.jp

Figure captions

Figure S1. HAADF-STEM images, EDX-mapping analysis, size distributions, and average sizes of catalysts. The green and yellow points in (b) correspond to Cu-L and Ag-L fluorescence lines, respectively.

Figure S2. TEM images, size distributions, and average sizes of Ag/Al$_2$O$_3$ before and after thermal aging at 900 °C for 100 h in air.

Figure S3. (a) Bright-field STEM image, (b) EDX-mapping analysis, and (c, d) HAADF-STEM images of CuO$_x$/Al$_2$O$_3$(aged). The blue and green points in (b) correspond to Al-K and Cu-L fluorescence lines, respectively. (d) Taken from the area shown by a black square in (a).[1]

Figure S4. High-magnification HAADF-STEM images of as-prepared Ag/Al$_2$O$_3$, CuO$_x$−Ag/Al$_2$O$_3$, and Ag/CuO$_x$/Al$_2$O$_3$.

Figure S5. Correlation between NH$_3$ combustion activity (T_{10}) and Ag–Ag coordination number for catalysts before and after thermal aging. Ag–Ag coordination number was estimated from Ag K-edge XAFS.

Figure S6. (left) Cu 2p and (right) Ag 3d XPS spectra of catalysts before and after thermal aging. The intensity of each spectrum was normalised by Al 2p.

Figure S7. Cu 2p and Ag 3d XPS depth profiles of as-prepared catalysts and Ag$_2$O as a reference. The intensity of each spectrum was normalised by Al 2p.

Figure S8. H$_2$-TPR profiles of supported catalysts before and after thermal aging, bulk materials, and support. H$_2$-TPR was performed in a flow system (5% H$_2$/Ar) at a constant rate of 10 °C·min^{-1}.

Figure S9. NH$_3$-TPD profiles of supports and catalysts before and after thermal aging. 5% NH$_3$/He, 10 °C·min^{-1}, *m/z* value of 15.

Figure S10. NO-TPD profiles of supports and catalysts before and after thermal aging. 1% NO/He, 10 °C·min^{-1}, *m/z* value of 30.

Figure S11. Product selectivities for catalytic NH$_3$ combustion over CuO$_x$/Ag/Al$_2$O$_3$ after thermal aging at 700 °C or 800 °C for 100 h in air. Reaction conditions: 1.0% NH$_3$, 1.5% O$_2$, λ = 2, He balance, W/F = 5.0 × 10^{-4} g·min·cm^{-3}.

Figure S12. Product selectivities for catalytic NH$_3$ combustion over binary catalysts before and after thermal aging at 900 °C for 100 h in air. Reaction conditions: 1.0% NH$_3$, 1.5% O$_2$, λ = 2, He balance, W/F = 5.0 × 10^{-4} g·min·cm^{-3}.

Figure S13. Product selectivities for the NH$_3$–NO–O$_2$ reaction over as-prepared catalysts. Reaction conditions: 0.8% NH$_3$, 0.2% NO, 1.4% O$_2$, He balance, W/F = 5.0 × 10^{-4} g·min·cm^{-3}.

MATERIALS AND METHODS

Characterization

XPS combined with depth profiling was conducted with Ar^+ ion beam bombardment (3000 eV), which was used for 10 s for each etch step. The C1s signal at 285.0 eV, derived from adventitious carbon, was used as a reference to correct the effect of surface charge.

Temperature-programmed reduction by H_2 (H_2-TPR) was performed in a flow system (5% H_2/Ar) at a constant rate of 10 °C·min^{-1}.

The calculation formulae of concentration ratios

For the NH_3–O_2 reaction (NH_3 combustion), the concentration ratios were calculated by the following formulae:

$$NH_3 = [NH_{3out}] / [NH_{3in}]$$

$$N_2O = 2[N_2O_{out}] / [NH_{3in}]$$

$$NO = [NO_{out}] / [NH_{3in}]$$

$$N_2 = 2[N_{2out}] / [NH_{3in}]$$

where $[NH_{3in}]$ is the inlet NH_3 concentration (1.0%) and $[NH_{3out}]$, $[N_2O_{out}]$, $[NO_{out}]$, and $[N_{2out}]$ are the outlet gas concentrations. N_2O and N_2 concentration ratios were doubled as 2 mol of nitrogen were present. The

formulae were approximated on the basis of the hypothesis that the volume of a gas mixture before and after reaction is invariable.

For the NH_3–NO–O_2 reaction, the concentration ratios were calculated by the following formulas:

$$NH_3 \quad = \quad [NH_{3out}] / ([NH_{3in}] + [NO_{in}])$$

$$N_2O \quad = \quad 2[N_2O_{out}] / ([NH_{3in}] + [NO_{in}])$$

$$NO \quad = \quad [NO_{out}] / ([NH_{3in}] + [NO_{in}])$$

$$N_2 \quad = \quad 2[N_{2out}] / ([NH_{3in}] + [NO_{in}])$$

where $[NH_{3in}]$ and $[NO_{in}]$ are the inlet NH_3 (0.8%) and NO concentrations (0.2%), respectively, and $[NH_{3out}]$, $[N_2O_{out}]$, $[NO_{out}]$, and $[N_{2out}]$ are the outlet gas concentrations. N_2O and N_2 concentration ratios were doubled as 2 mol of nitrogen were present.

CuO$_x$/Ag/Al$_2$O$_3$

Cu-L   Ag-L
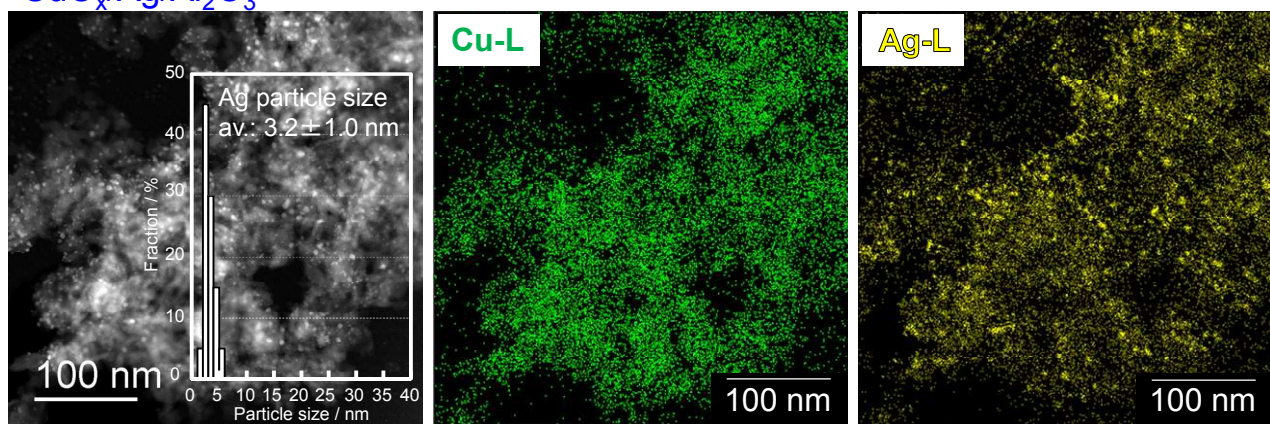
CuO$_x$/Ag/Al$_2$O$_3$(900 °C)
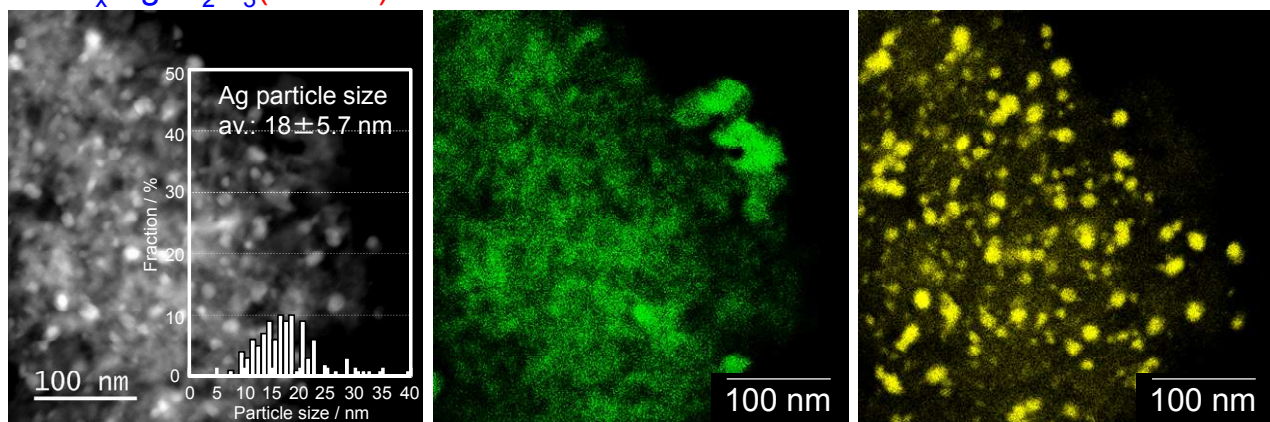
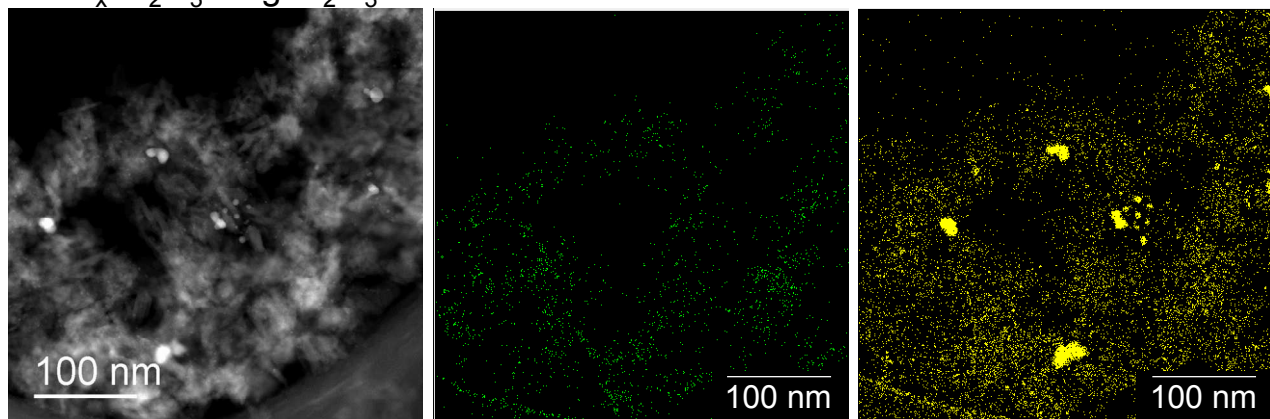CuO$_x$/Al$_2$O$_3$ + Ag/Al$_2$O$_3$

Figure S1. HAADF-STEM images, EDX-mapping analysis, size distributions, and average sizes of catalysts.

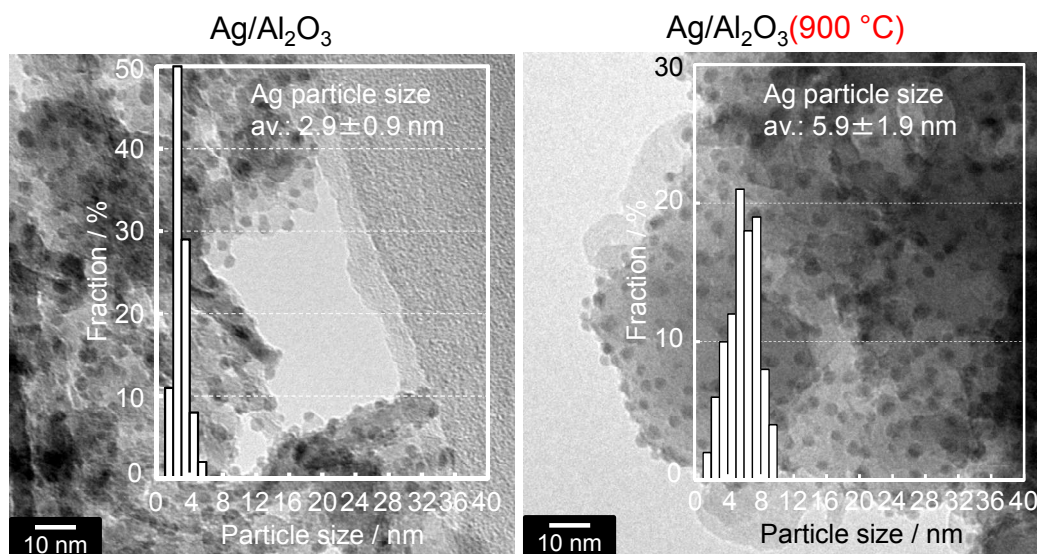The green and yellow points in (b) correspond to Cu-L and Ag-L fluorescence lines, respectively.

Figure S2. TEM images, size distributions, and average sizes of Ag/Al$_2$O$_3$ before and after thermal aging at 900 °C for 100 h in air.
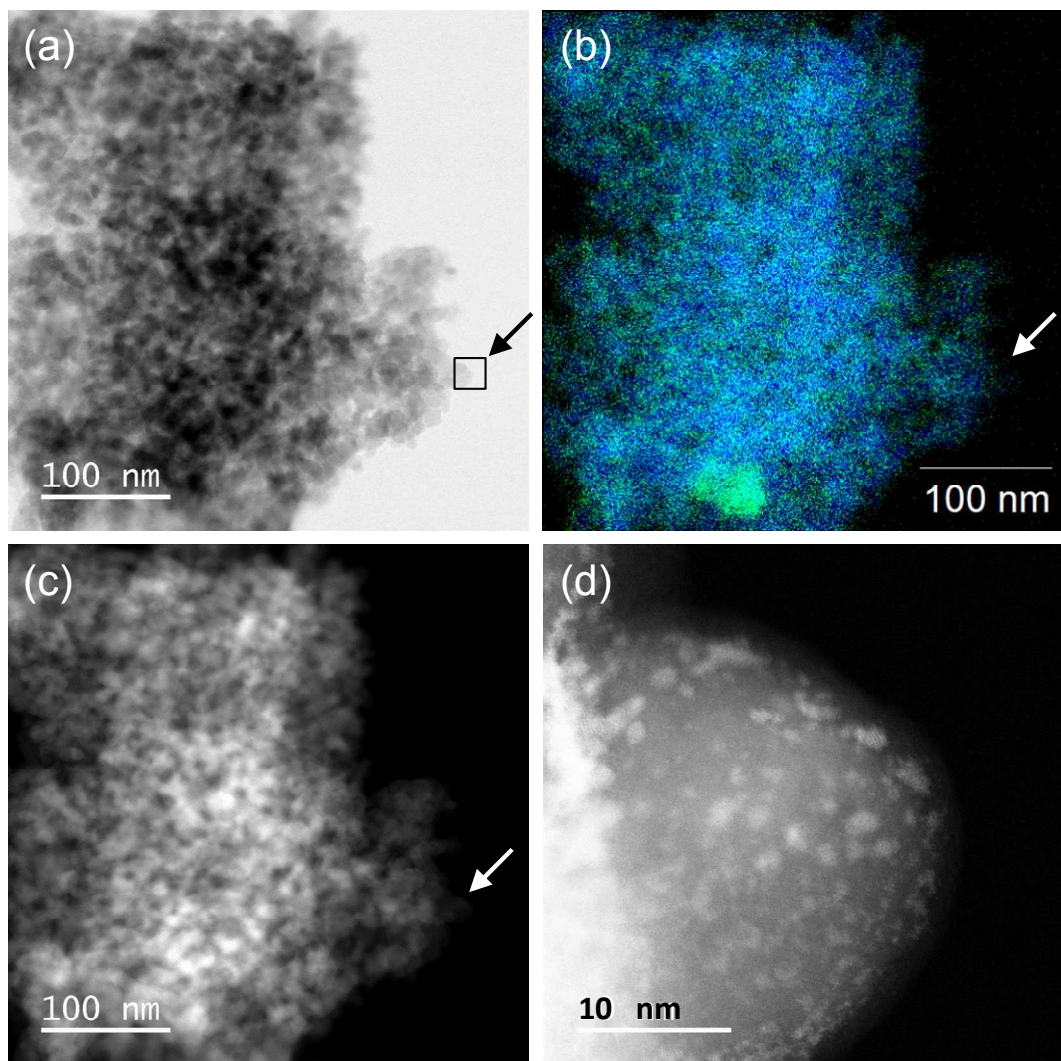
Figure S3. (a) Bright-field STEM image, (b) EDX-mapping analysis, and (c, d) HAADF-STEM images of

CuO_x/Al_2O_3(aged). The blue and green points in (b) correspond to Al-K and Cu-L fluorescence lines,

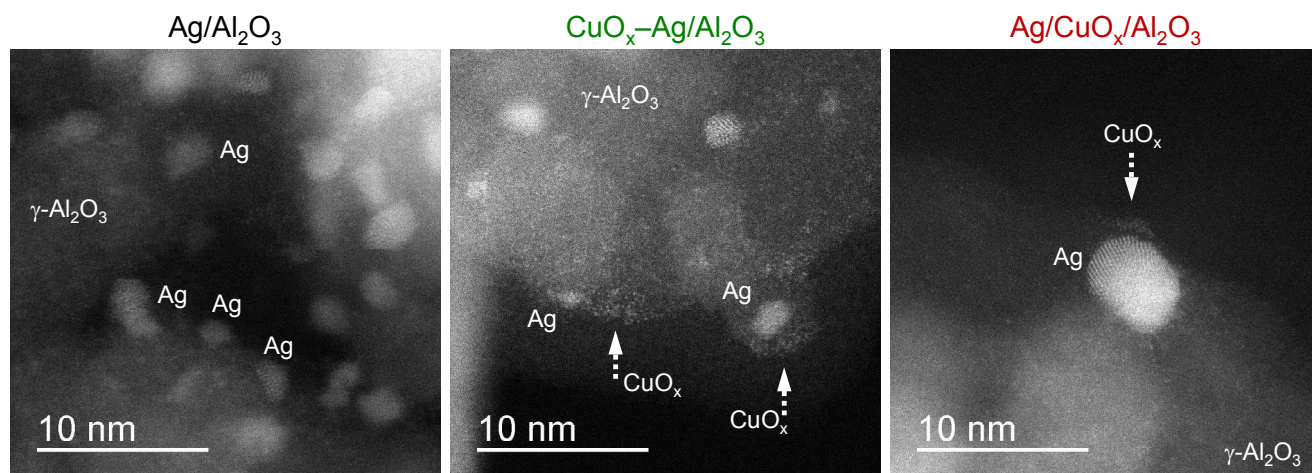respectively. (d) Taken from the area shown by a black square in (a).[1]

Figure S4. High-magnification HAADF-STEM images of as-prepared Ag/Al$_2$O$_3$, CuO$_x$−Ag/Al$_2$O$_3$, and Ag/CuO$_x$/Al$_2$O$_3$.
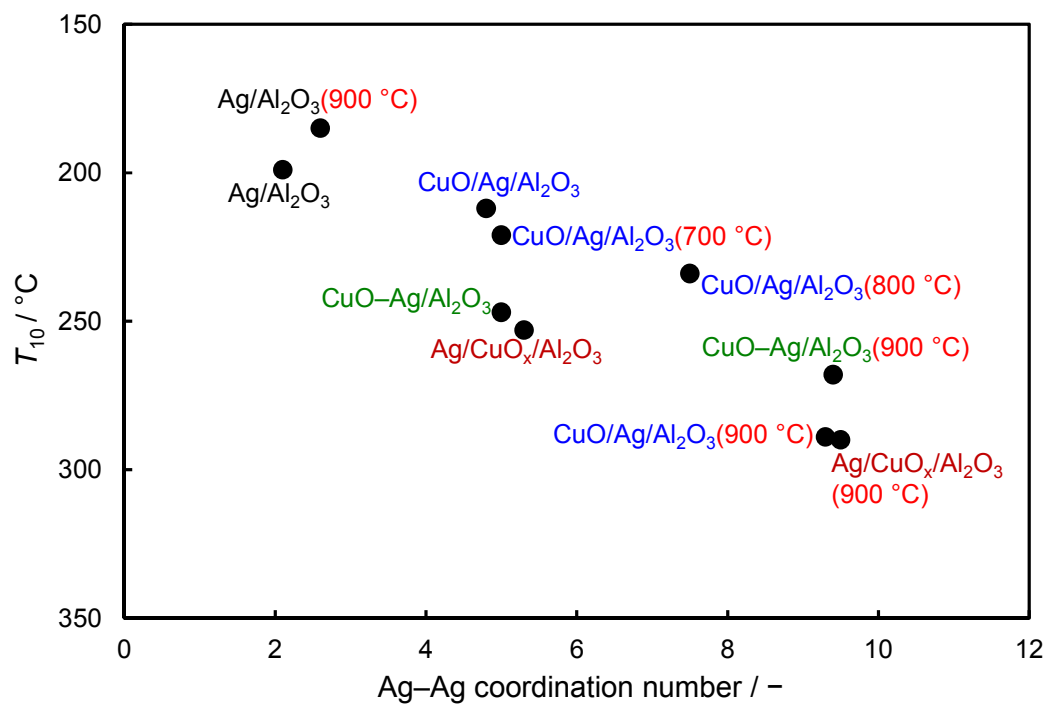
Figure S5. Correlation between NH_3 combustion activity (T_{10}) and Ag–Ag coordination number for catalysts before and after thermal aging. Ag–Ag coordination number was estimated from Ag K-edge XAFS.
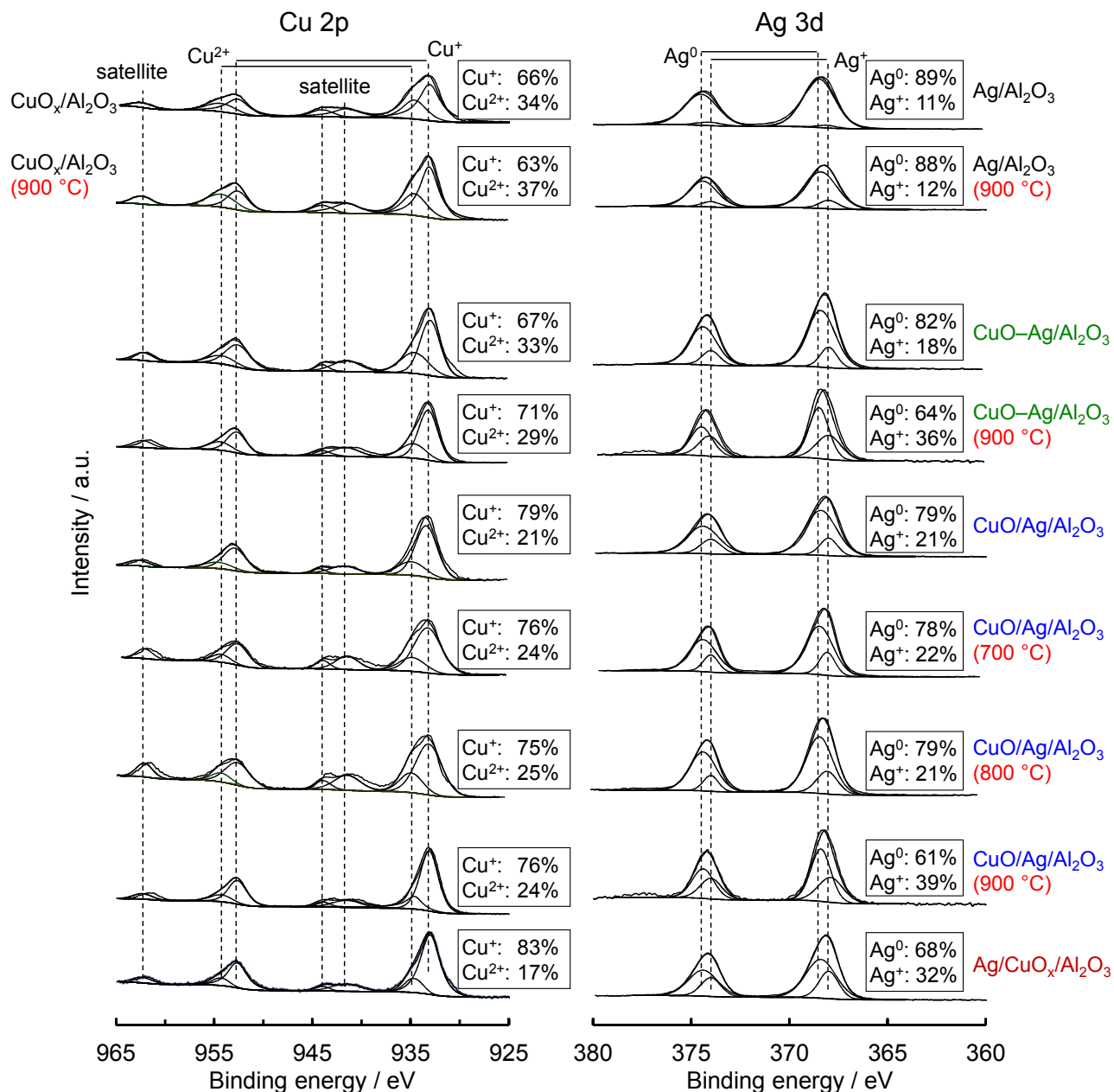
Figure S6. (left) Cu 2p and (right) Ag 3d XPS spectra of catalysts before and after thermal aging. The intensity of each spectrum was normalised by Al 2p.

The Cu 2p XPS spectra of the catalysts exhibit two Cu $2p_{3/2}$ peaks assignable to Cu$^+$ and Cu^{2+} at 933.1 and 934.6 eV, respectively. Additionally, two satellite peaks (941.5 and 944.0 eV), attributed to Cu^{2+} with the $3d^9$ electronic state, are also found. Unlike the thermodynamically stable Cu^{2+} in atmosphere, Cu$^+$ is

observed in all catalysts, which is indicative of highly dispersed CuO_x nanoparticles (Figure 4 and Supporting Information) having a high fraction of surface CuO_x species with lower oxygen coordination numbers than bulk CuO_x (Cu^{2+}). Based on previous reports,[2,3] in the case of the Ag 3d XPS spectra, the deconvolution of the observed peaks reveals two sets of spin-orbital doublets assigned to Ag^0 and Ag^+. Al 2p and/or O 1s XPS spectra of these catalysts were also measured; however, no noticeable difference was observed.
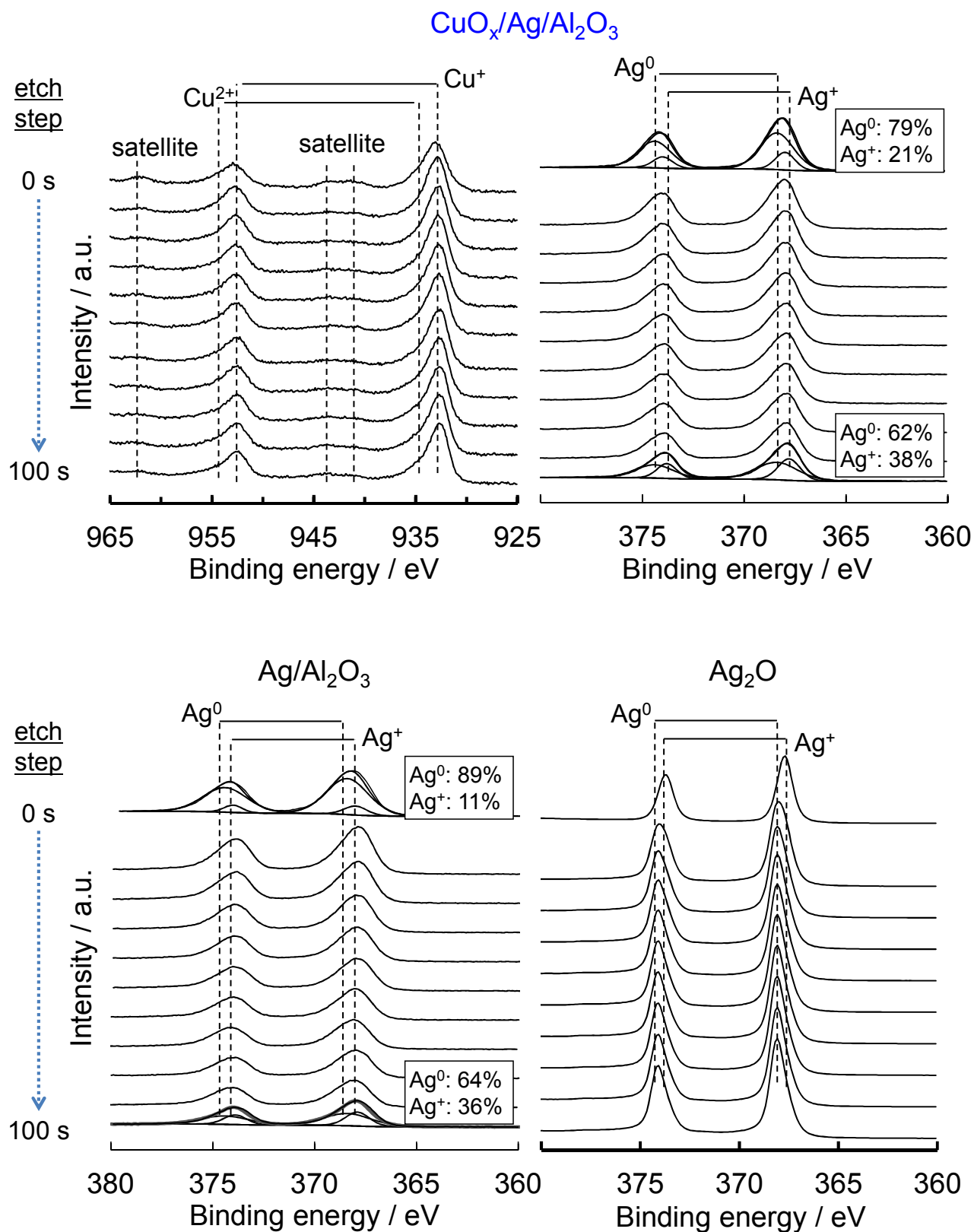
Figure S7. Cu 2p and Ag 3d XPS depth profiles of as-prepared catalysts and Ag$_2$O as a reference. The intensity of each spectrum was normalised by Al 2p.

Unlike the Ag 3d XPS depth profiles for as-prepared $CuO_x/Ag/Al_2O_3$ and Ag/Al_2O_3, that for bulk Ag_2O shows that the fraction of Ag^0 increases with increasing etch step, which implies that Ag_2O is reduced to metallic Ag (Ag^0) by the Ar^+ ion beam. Conversely, the Cu 2p peaks for $CuO_x/Ag/Al_2O_3$ shift slightly to lower binding energy (from Cu^{2+} to Cu^+) with increasing etch step. It is also thought that the CuO_x nanoparticles in $CuO_x/Ag/Al_2O_3$ are reduced by the Ar^+ ion beam.
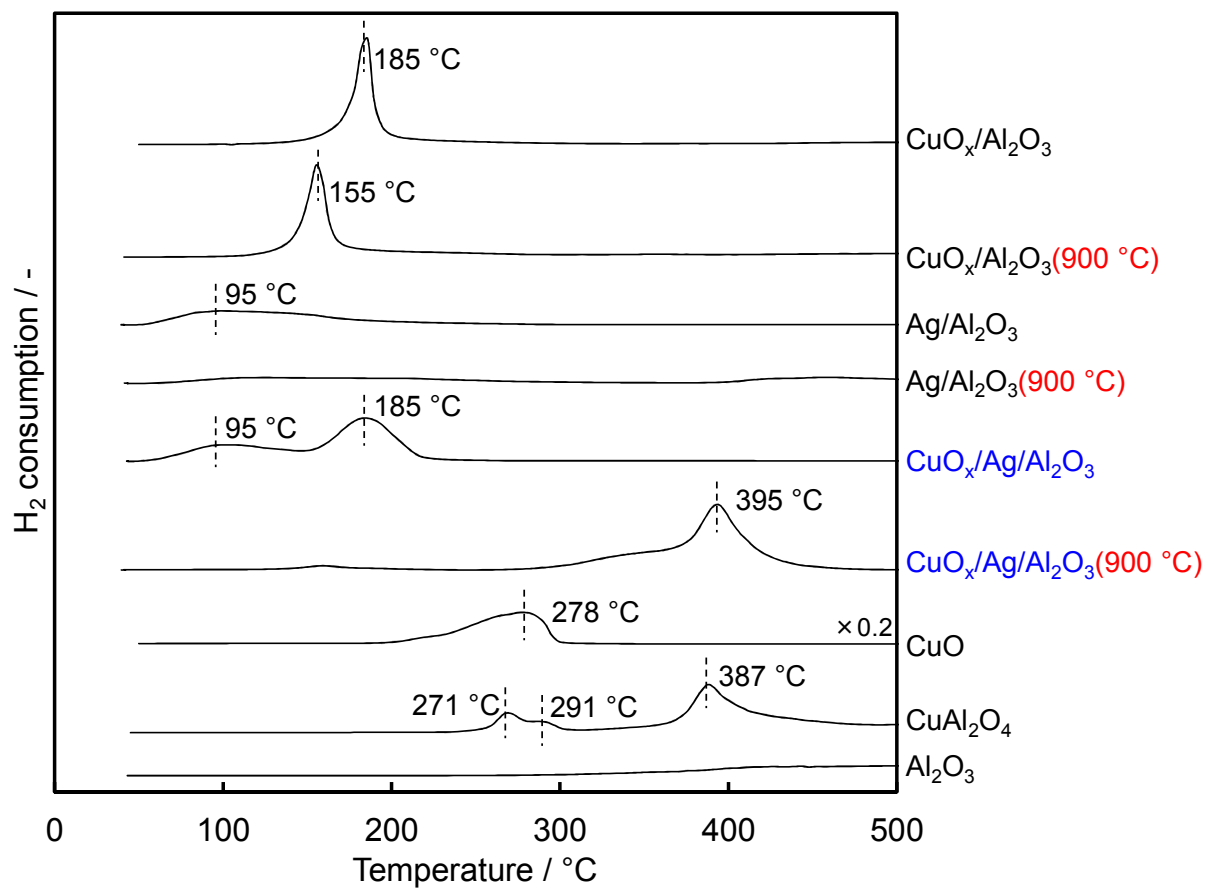
Figure S8. H_2-TPR profiles of supported catalysts before and after thermal aging, bulk materials, and support. H_2-TPR was performed in a flow system (5% H_2/Ar) at a constant rate of 10 °C·min^{-1}.
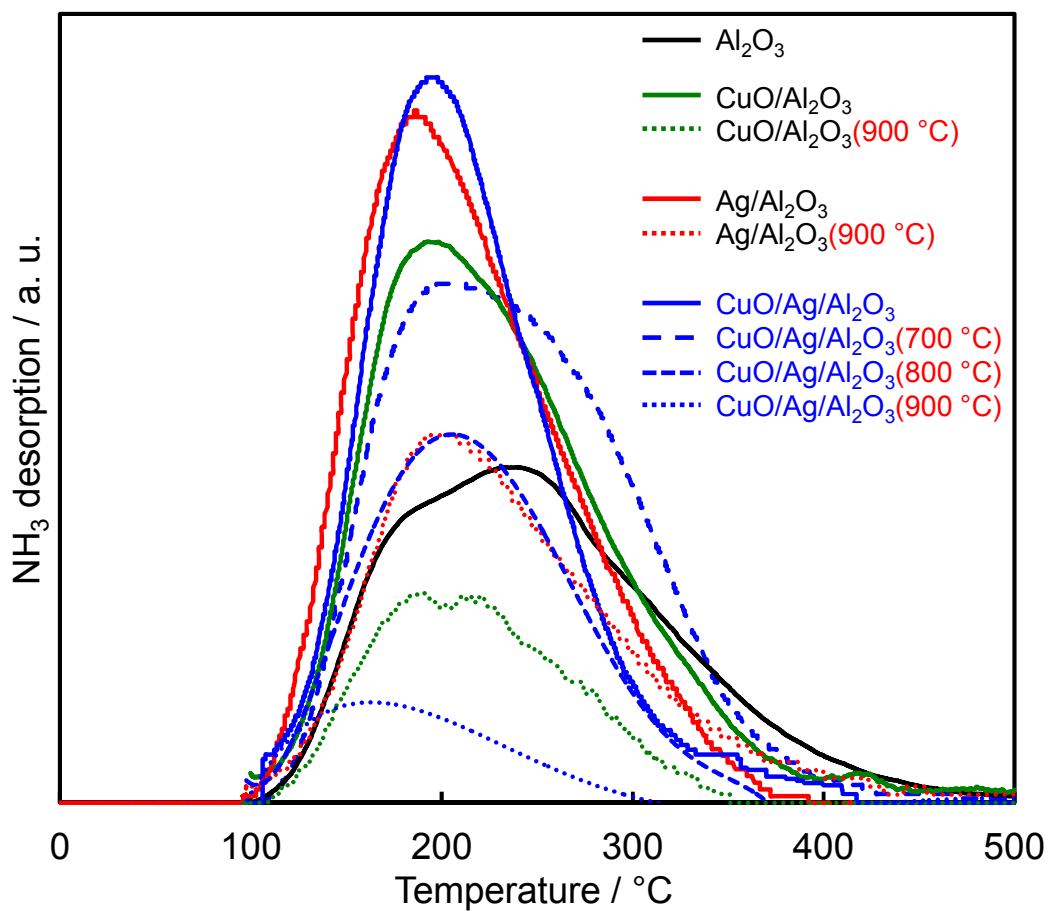
Figure S9. NH$_3$-TPD profiles of supports and catalysts before and after thermal aging. 5% NH$_3$/He, 10 °C·min^{-1}, *m/z* value of 15.
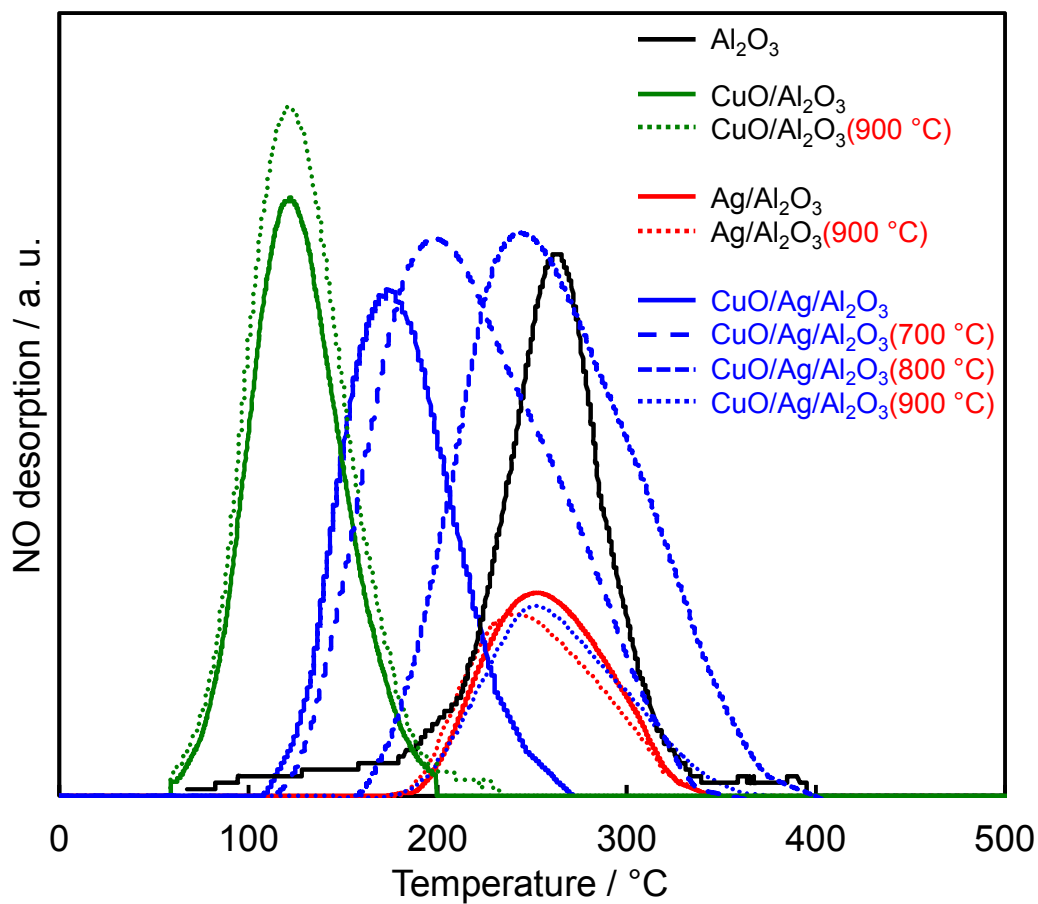
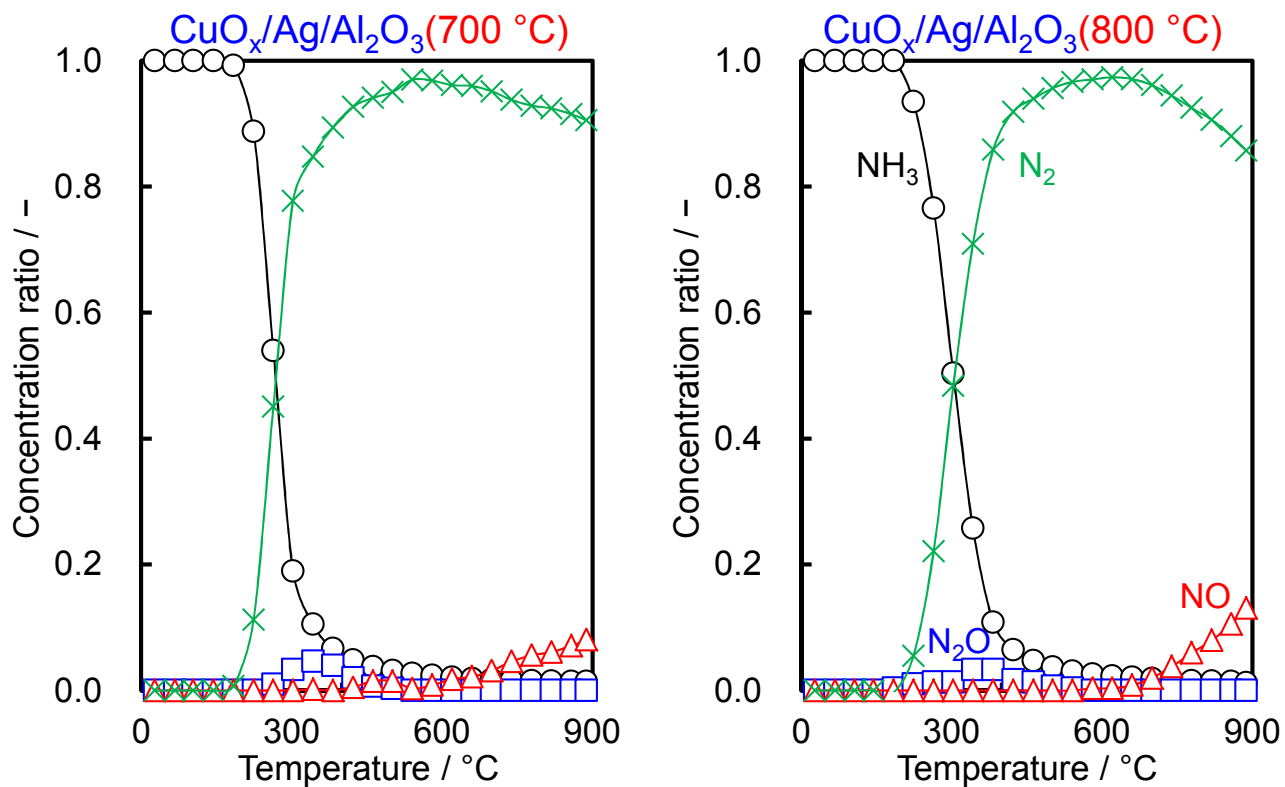**Figure S10.** NO-TPD profiles of supports and catalysts before and after thermal aging. 1% NO/He, 10 °C·min^{-1}, m/z value of 30.

Figure S11. Product selectivities for catalytic NH_3 combustion over $CuO_x/Ag/Al_2O_3$ after thermal aging at 700 °C or 800 °C for 100 h in air. Reaction conditions: 1.0% NH_3, 1.5% O_2, $\lambda = 2$, He balance, W/F = 5.0 $\times$ 10^{-4} g·min·cm^{-3}.
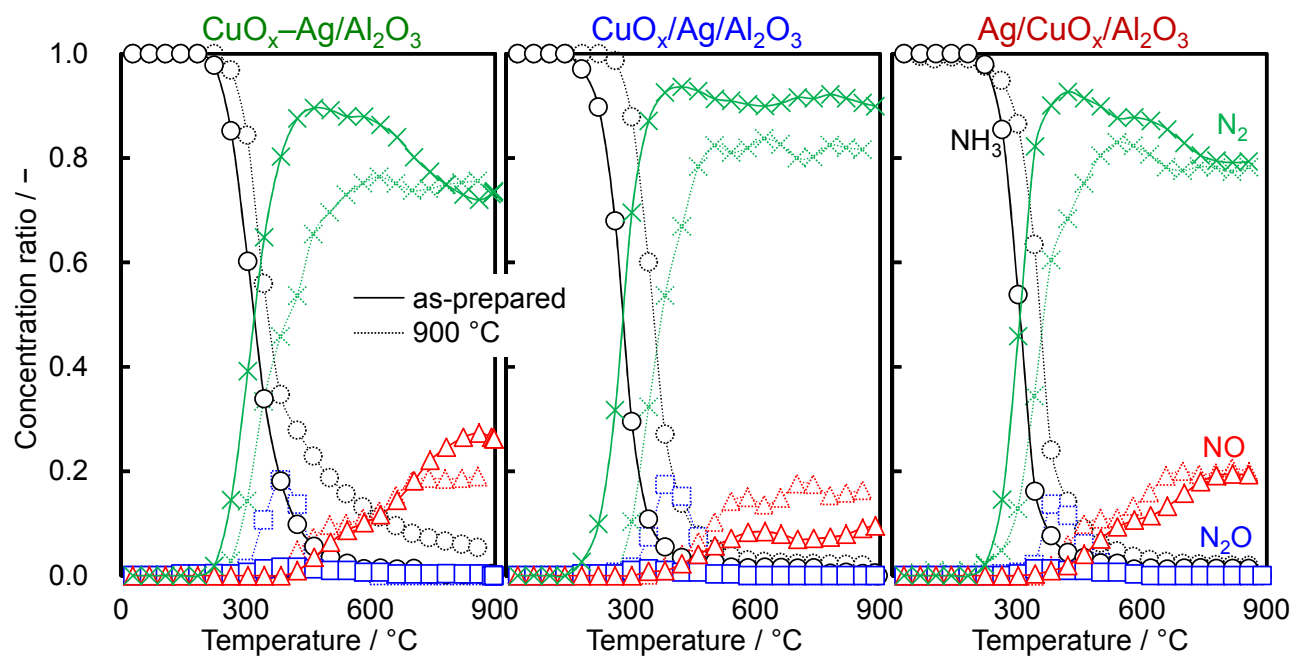
Figure S12. Product selectivities for catalytic NH$_3$ combustion over binary catalysts before and after thermal aging at 900 °C for 100 h in air. Reaction conditions: 1.0% NH$_3$, 1.5% O$_2$, λ = 2, He balance, W/F = 5.0 × 10^{-4} g·min·cm^{-3}.
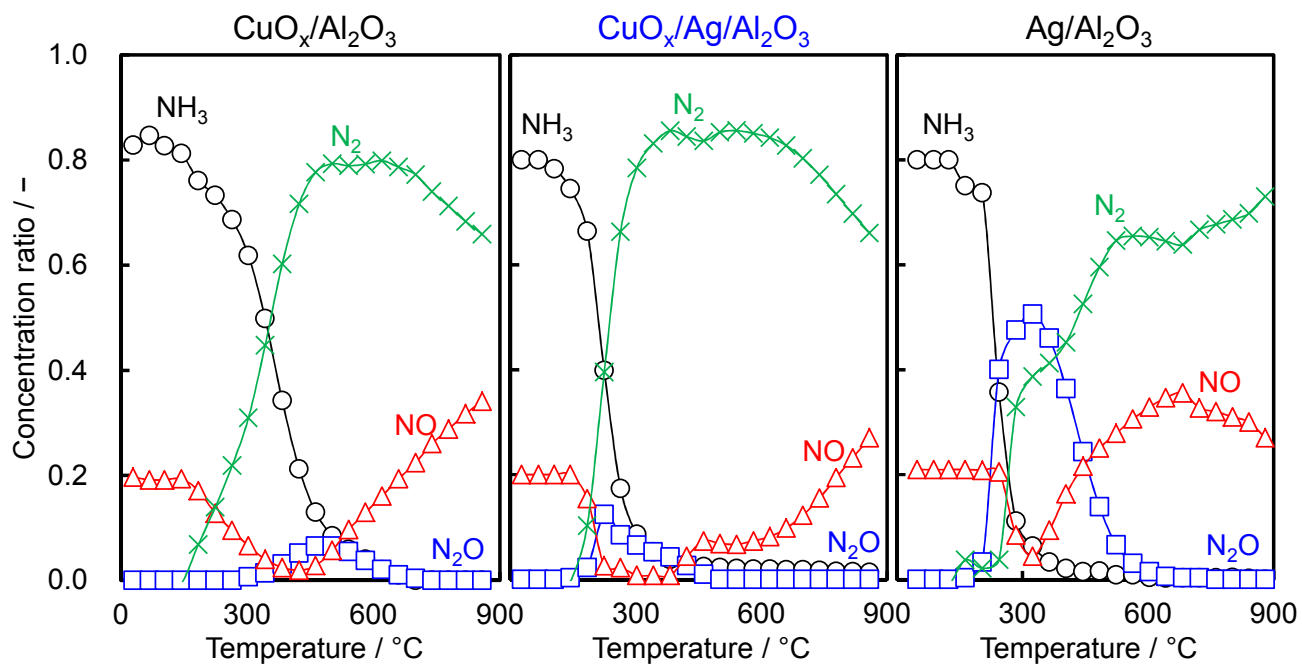
Figure S13. Product selectivities for the NH_3–NO–O_2 reaction over as-prepared catalysts. Reaction conditions: 0.8% NH_3, 0.2% NO, 1.4% O_2, He balance, W/F = 5.0×10^{-4} g·min·cm^{-3}.

REFERENCES

(1) Hinokuma, S.; Matsuki, S.; Kawabata Y.; Shimanoe, H.; Kiritoshi S.; Machida, M. Copper Oxides Supported on Aluminum Oxide Borates for Catalytic Ammonia Combustion. *J. Phys. Chem. C.* **2016**, *120*, 24734–24742.

(2) Kuo, Y.; Chen, H.; Ku, Y., Analysis of Silver Particles Incorporated on TiO_2 Coatings for the Photodecomposition of O-cresol. *Thin Solid Films* **2007**, *515*, 3461–3468.

(3) Sohn, Y., SiO_2 Nanospheres Modified by Ag Nanoparticles: Surface Charging and CO Oxidation Activity. *J. Mol. Catal. A: Chem.* **2013**, *379*, 59–67.